

Fernando I. Gómez-Castro¹
Juan Gabriel Segovia-
Hernández¹
Salvador Hernández¹
Claudia Gutiérrez-Antonio²
Abel Briones-Ramírez^{3,4}

Research Article

Dividing Wall Distillation Columns: Optimization and Control Properties

The optimal design of dividing wall columns is a non-linear and multivariable problem, and the objective function used as optimization criterion is generally non-convex with several local optimums. Considering this fact, in this paper, we studied the design of dividing wall columns using as a design tool, a multi-objective genetic algorithm with restrictions, written in MatlabTM and using the process simulator Aspen PlusTM for the evaluation of the objective function. Numerical performance of this method has been tested in the design of columns with one or two dividing walls and with several mixtures to test the effect of the relative volatilities of the feed mixtures on energy consumption, second law efficiency, total annual cost, and theoretical control properties. In general, the numerical performance shows that this method appears to be robust and suitable for the design of sequences with dividing walls.

Keywords: Columns – Dividing wall, Design, Energy consumption, Optimization

Received: February 27, 2008; *revised:* April 01, 2008; *accepted:* April 04, 2008

DOI: 10.1002/ceat.200800116

¹ Universidad de Guanajuato,
Facultad de Química,
Guanajuato, México.

² CIATEQ, A.C., Querétaro,
México.

³ Instituto Tecnológico de
Aguascalientes, Departamento
de Ingeniería Química,
Aguascalientes, México.

⁴ Innovación Integral de
Sistemas S.A. de C.V.,
Querétaro, México.

1 Introduction

At present, distillation remains one of the most widely used separation methods in the chemical engineering industry. However, this separation process conveys a significant disadvantage: it requires high amounts of energy. In fact, the cost of steam has the highest contribution to the total annual cost of a distillation column. Moreover, the distillation process has inherent low thermodynamic efficiency. Several attempts have been made to reduce energy consumption in distillation sequences. Some research efforts have addressed the integration of distillation columns with the overall process [1, 2], which can give significant energy savings. Other efforts focus on the development of complex structures such as thermally coupled distillation sequences, consisting of the implementation of vapor-liquid interconnections, achieving heat transfer by direct contact between the streams of the columns, and resulting in the elimination of condensers and/or reboilers of the columns. Through an appropriate selection of operating conditions, these systems can produce significant energy savings over conventional distillation sequences. For ternary mixtures, there are three sequences especially studied by many researchers [3, 4], namely: the thermally coupled system with a

side rectifier (TCDS-SR, Fig. 1a)), the thermally coupled system with a side stripper (TCDS-SS, Fig. 1b)), and the Petlyuk column (Fig. 1c)). Theoretical studies [5–7] have shown that distillation schemes with side columns typically have energy savings of 30 % over conventional schemes.

In industrial applications, the Petlyuk scheme is equivalent to the dividing wall column (DWC). The DWC offers the possibility of both energy and capital cost savings. The capital cost savings result from the reduction in quantity of equipment (i.e., one shell instead of two in the case of the Petlyuk column). There are also indirect benefits: a DWC requires less plot area, and therefore, shorter piping and electrical runs. Flare loads are reduced because of the lower heat input and smaller fire-case surface, leading to a smaller flare system [8].

Recently, Kim [9] proposed a Petlyuk-like scheme which includes a postfractionator (i.e., a column with two dividing walls), establishing that this sequence can achieve lower energy consumption than the Petlyuk column in some cases.

An important issue in the design of DWCs is their dynamic properties. A good design may show energy savings but lack good controllability. For many years, DWCs were considered problematic schemes because of the presence of recycle streams. Nevertheless, many studies [10–17] have shown that control properties of integrated sequences can be better than those of conventional sequences, in many cases. In other words, it is possible to have both total annual cost savings and good dynamic performance.

There have been many attempts to develop a useful design methodology for DWCs. An ideal method is one that combines easy implementation (low mathematical effort) and a

Correspondence: Prof. J. G. Segovia-Hernández (gsegovia@quijote.ugto.mx), Universidad de Guanajuato, Facultad de Química, Noria Alta s/n, Guanajuato, Gto., México 36050.

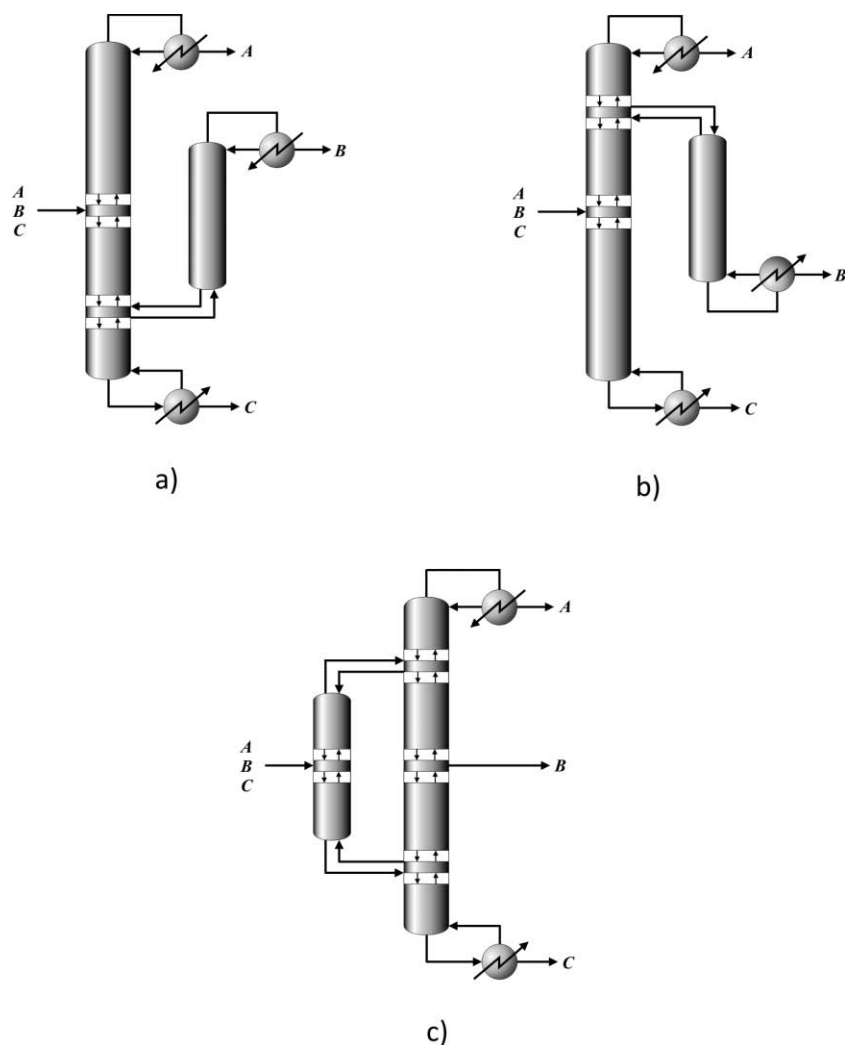


Figure 1. Thermally coupled distillation sequences: (a) TCSD with a side rectifier (TCDS-SR), (b) TCSD with a side stripper (TCDS-SS), (c) the Petlyuk column.

good approach to the global optimum of energy consumption. In chemical engineering, various calculations can be formulated as optimization problems with or without restrictions. Some examples of these calculations are phase stability analysis, phase equilibrium problems, parameter estimation in thermodynamic models, calculation of critical points, and processes synthesis. Generally, these problems are non-linear and multivariable, and the objective function used as optimization criterion is non-convex with several local optimums. As a consequence, solving with local optimization methods is not reliable because they generally converge to local optimums. One example of this is the method proposed by Hernandez and Jimenez [18]. In this method, a design based on conventional distillation sequences is considered. In order to determine the structures of the thermally coupled distillation columns, sections of the conventional sequence are moved to obtain the new sequence, and then by a parametric search, a zone with a minimal heat duty is found. The problem with this

method, as referred to before, is that it is easy to fall into a local optimum.

As described by Henderson et al. [19], the formulation of chemical engineering calculations for optimization problems offers several advantages: a) the use of a robust optimization method, b) the possibility of using a direct optimization method which only requires calculations of the objective function, and c) the use of an iterative procedure whose convergence is almost independent from the initial guesses. During recent years, the development and application of global optimization strategies has increased in many areas of chemical engineering. Global optimization methods can be classified as deterministic and stochastic. The first class offers a guarantee of finding the global optimum of the objective function, provided that the objective function is convex. However, these strategies often require high computation time (generally more time than stochastic methods), and in some cases, problem reformulation is necessary. On the other hand, stochastic optimization methods are robust numerical tools that present a reasonable computational effort in the optimization of multivariable functions; they are applicable to ill-structured or unknown structure problems and can be used with all thermodynamic models.

With regards to deterministic optimization, several methods have been developed [20–23] proposing the use of superstructures for optimum design of distillation sequences. These methods are able to achieve the global minimum on energy consumption, but they demand high mathematical efforts. Furthermore, the formulation of such models is difficult

and time consuming. In addition to the time and expertise needed to formulate these models, the synthesis and design of distillation sequences pose other difficulties. The use of rigorous design and thermodynamic models leads to very large non-convex models, which are very difficult to converge. Moreover, taking into account structural and design decisions such as the existence of stages, columns, condensers, and reboilers lead to the inclusion of integer variables which further increase the difficulty of solving the model. Finally, additional convergence problems are generated when discontinuous functions, such as complex cost functions, are introduced in the model. To compensate for these difficulties, it is often necessary to supply initial values for the optimization variables very close to the actual solution, something that is not always an easy task. Even recent studies have employed simplifications for the design model, thermodynamics, hydraulics, or cost functions to obtain feasible solutions or to examine complex superstructures in synthesis problems [24].

On the other hand, in the case of stochastic optimization, there are methods known as genetic algorithms (GA), which are a part of the wider field of evolutive algorithms. These algorithms were first proposed by Holland [25] to solve optimization problems. Genetic algorithms are stochastic methods based on the idea of evolution and survival of the fittest. In a GA, a set of values for the optimization variables forms an individual, usually codified in a chromosome through a series of bits (0–1). The algorithm begins by generating a random population (a group of individuals), and then repetitively evolves it with three basic genetic operators: selection, crossover, and mutation. For a detailed explanation of genetic algorithms and operators, the reader is referred to the classic book by Goldberg [26] or the book by Gen and Cheng [27]. Many studies [24, 28–30] have been conducted, applying genetic algorithms to design in chemical engineering. In 2007, Gutiérrez-Antonio [32] used genetic algorithms to solve optimization problems for azeotropic distillation, without the above mentioned numerical problems. Genetic algorithms have several features that make them attractive for solving optimization problems with modular simulators, where the model of each unit is only available in an implicit form (black-box model). First, due to the fact that they are based on a direct search method, it is not necessary to have explicit information on the mathematical model or its derivatives. Secondly, the search for the optimal solution is not limited to one point but rather relies on several points simultaneously, therefore the knowledge of initial feasible points is not required and such points do not influence the final solution.

Other developments using stochastic multi-objective mixed integer dynamic optimization for batch distillation has been presented by Barakat et al. [31].

In this paper, we studied the design of three schemes with dividing walls [Petlyuk column (PTLK), Petlyuk with postfractionation system (PTLKP) and two-wall column (APTLK); Fig. 2] using as a design tool, a multi-objective genetic algorithm with restrictions coupled with the process simulator, Aspen PlusTM, for the evaluation of the objective function, ensuring that all results obtained are rigorous. Numerical performance of this method was tested in the design of columns with one and two dividing walls, and with several mixtures to examine the effect of the relative volatilities of the feed mixtures. The study is complemented by a dynamic analysis of the structures obtained with the algorithm. In general, numerical performance shows that this method appears to be robust and suitable for the design of complex distillation sequences (with dividing wall).

2 Design Tool: Genetic Algorithm

The tool implemented was used to rigorously design and optimize the dividing wall columns, and is briefly described here; for more information, the reader is referred to the work by Gutiérrez-Antonio [32].

We can say that a point in the search space is considered to be the Pareto optimum if there is no feasible vector that can decrease the value of one objective without simultaneously increasing the value of another objective in the case of minimi-

zation. Now, we define that \vec{x} dominates \vec{y} when $f(\vec{x}) < f(\vec{y})$, if $Y \subseteq \mathfrak{S}$ and $\vec{y} \in Y^{1)}$. If none $\vec{x} \in Y$ dominates \vec{y} , we say that \vec{y} is not dominated with respect to Y . The set of solutions not dominated that are optimums of Pareto is the Pareto front [32].

Thus, the Pareto front represents all optimal designs, from minimum number of stages (infinite reflux ratio) to minimum reflux ratio (infinite number of stages). This set of optimal solutions allows the engineer to choose a good compromise between the two goals by picking a point somewhere along the Pareto front.

For the specific problem of optimization of the Petlyuk sequence, the minimization of heat duty, Q , and the number of stages of the sequence, N_i , can be expressed as:

$$\begin{aligned} \text{Min}(Q, N_i) &= f(Q, R, N_i, N_j, N_s, N_F, F_j) \\ \text{st} & \\ \vec{y}_k &\geq \vec{x}_k \end{aligned} \quad (1)$$

where R is the reflux ratio, N_i is the total number of stages of column i , N_j is the stage of the flow of interconnection stream j , N_s is the side stream stage, N_F is the feed stage, F_j is the flow of interconnection stream j , and \vec{x}_k and \vec{y}_k are the vectors of purities required and obtained, respectively. We observe that the two variables in competition, Q and N_i , are involved in the optimization problem.

For this minimization, the implemented multi-objective algorithm is based on the NSGA-II and handling constraints using a slight modification of the work by Coello [33]. This slight modification is as follows: The entire population is divided into sub-populations using, as criterion, the total number of satisfied constraints. Thus, the best individuals of the generation are those that satisfied the n constraints, and they are followed by the individuals only satisfying $n - 1$, and so on. Within each sub-population, individuals are ranked using the NSGA-II, but considering now as other objective function to minimize, the degree of unsatisfied constraints. Next, dominance calculation of each subgroup is carried out as follows:

$$\{Q, N_i, \min[0, (\vec{x}_k - \vec{y}_k)]\} \quad (2)$$

The idea behind this is minimizing for each subgroup as the original objective function as the amount of violated constraints.

For the purpose of this paper, we choose the best trade-off solution between energy and the number of stages of the sequence, in order to study the dynamic properties of the dividing wall columns. This best trade-off solution is found when an increase in reflux ratio does not correspond to a significant decrease in the number of stages. Fig. 3 shows a block diagram for the genetic algorithm.

1) List of symbols at the end of the paper.

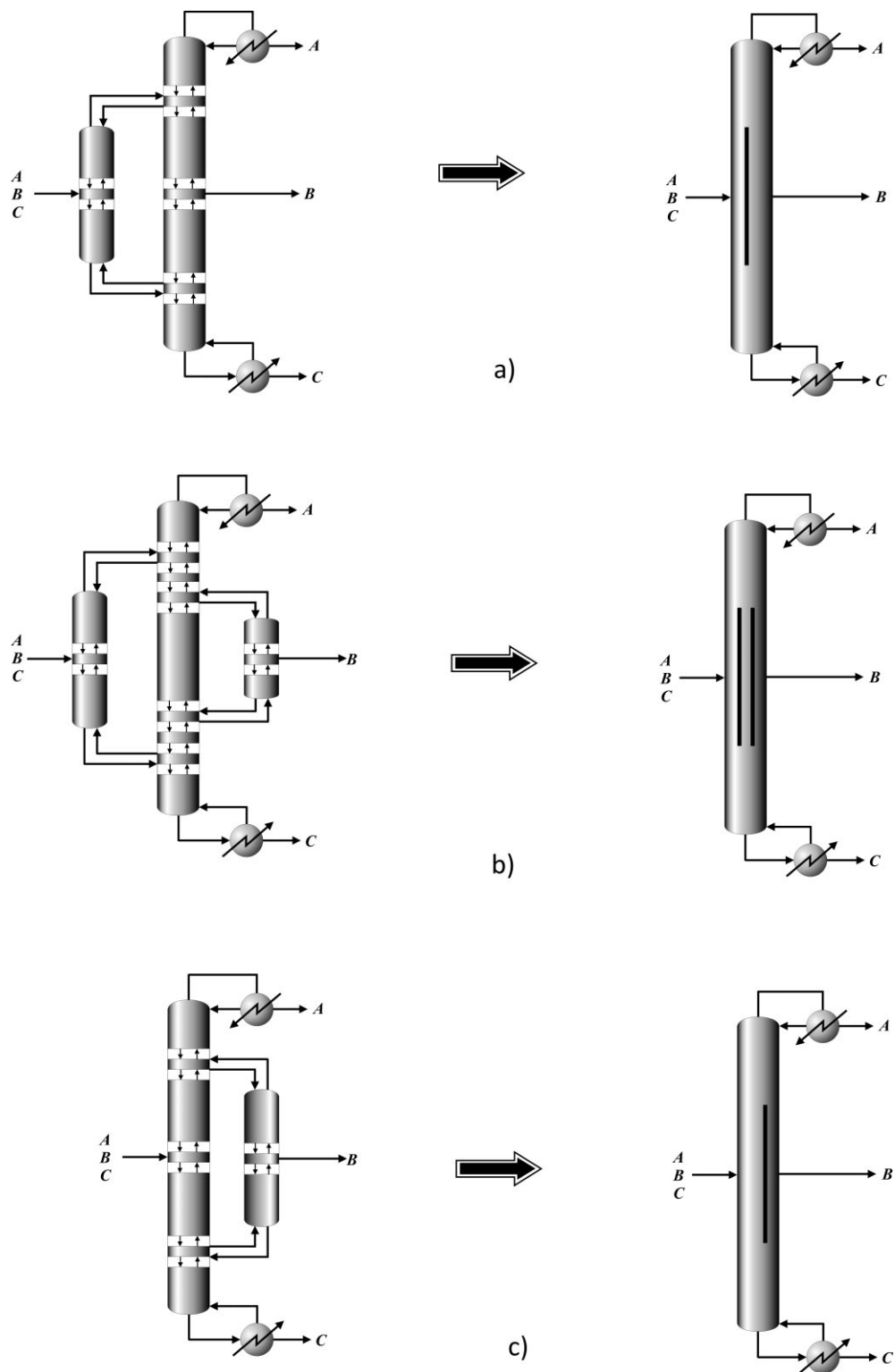


Figure 2. (a) Petlyuk column (PTLK) and dividing wall column, (b) Petlyuk with postfractionator system (PTLKP) and two-wall column, (c) Alternative Petlyuk column (APTLK) and dividing wall column.

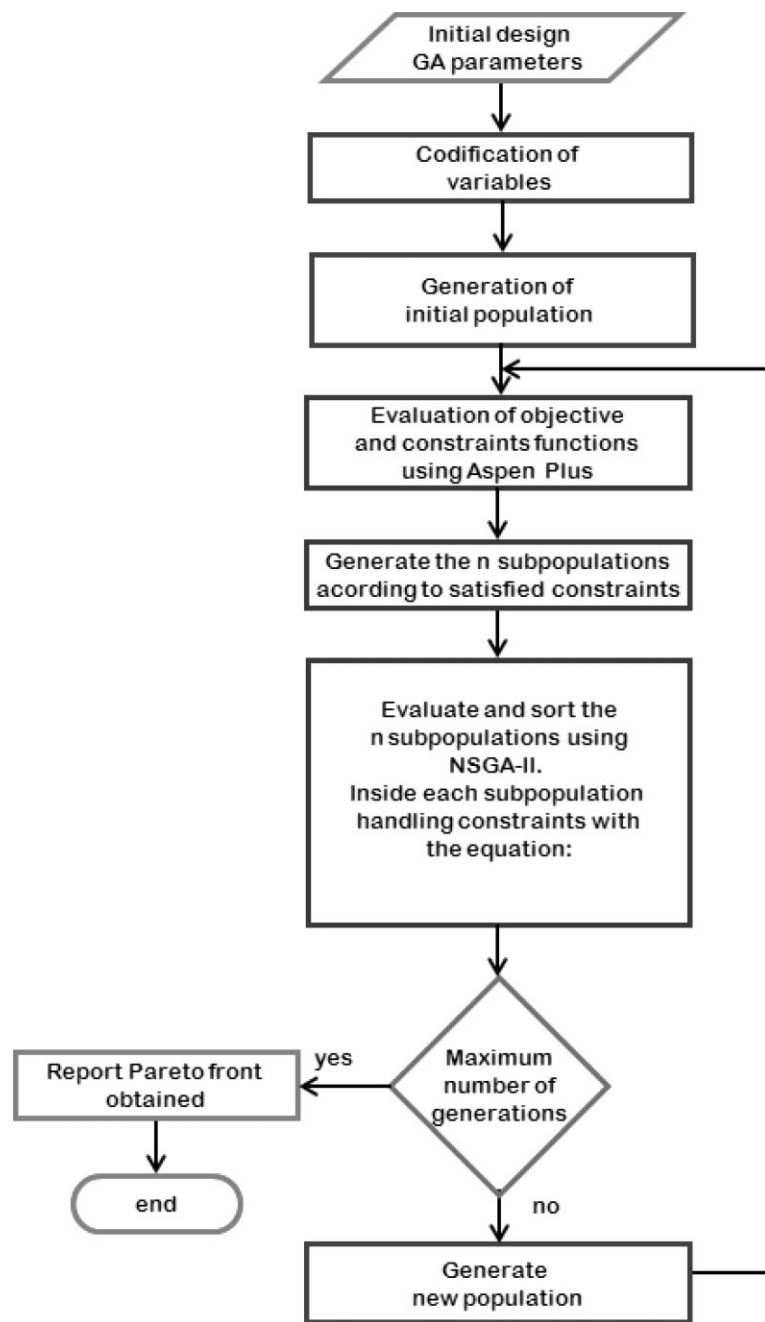


Figure 3. Block diagram for the genetic algorithm.

3 Control Properties (Singular Value Decomposition)

One important use of singular value decomposition (SVD) is in the study of theoretical control properties in chemical process. One definition of SVD is:

$$G = V \Sigma W^H \quad (3)$$

Here, G is the matrix target for SVD analysis, Σ is a diagonal matrix which consists of the singular values of G , V is a matrix which contains the left-singular vector of G , and W is the matrix composed of the left-singular vectors of G (more details about the mathematical basis in Klema and Laub [34]).

Where SVD is used for the study of theoretical control properties, two parameters are of interest: the minimum singular value (σ^*), the maximum singular value (σ^+), and the ratio of the two values known as the condition number (γ):

$$\gamma = \frac{\sigma^+}{\sigma^*} \quad (2)$$

The minimum singular value is a measure of the invertibility of the system and provides evidence of potential problems of the system under feedback control. The condition number reflects the sensitivity of the system to uncertainties in process parameters and modeling errors. These parameters provide a qualitative assessment of theoretical control properties of alternate designs. The systems with higher minimum singular values and lower condition numbers are expected to show the best dynamic performance under feedback control [34–35]. Also, it is important to note that a full SVD analysis should cover a wide range of frequencies. The SVD technique requires a transfer function matrix (G in Eq. (3)) around the optimum design of the distillation sequences. For the distillation sequences presented in this study, three controlled variables were considered, product composition, A , B , C . Similarly, three manipulated variables were defined, reflux ratios (R_i), heat duties supplied to reboilers (Q_j), and side stream flowrate (L).

4 Case Study

To compare the steady and dynamic performance of the sequences, three ternary mixtures with different ease of separability index values ($ESI = a_{AB}/a_{BC}$), as defined by Tedder and Rudd [36] were considered. The mixtures studied are described in Tab. 1; the feed flowrate was 45.36 kmol/h. The design pressure for each separation was chosen to ensure the use of cooling water in the condensers. It is well known that energy savings obtained in coupled structures for ternary separations strongly depend on the amount of intermediate component. For that reason, two feed compositions were assumed for each mixture with a low or high content of the intermediate component.

5 Results

The results are presented in two sections. In the first section, the three thermally coupled distillation sequences are com-

Table 1. Mixtures Analyzed.

Mixture	Components	Feed Composition (Mole Fraction)
M1F1	<i>n</i> -butane, <i>n</i> -pentane, <i>n</i> -hexane	0.40, 0.20, 0.40
M1F2	<i>n</i> -butane, <i>n</i> -pentane, <i>n</i> -hexane	0.15, 0.70, 0.15
M2F1	<i>n</i> -butane, isopentane, <i>n</i> -pentane	0.40, 0.20, 0.40
M3F1	isopentane, <i>n</i> -pentane, <i>n</i> -hexane	0.40, 0.20, 0.40
M4F1	benzene, toluene, ethylbenzene	0.40, 0.20, 0.40
M5F1	toluene, ethylbenzene, <i>o</i> -xylene	0.40, 0.20, 0.40

Table 2. Design variables, M1F1, Petlyuk (PTLK).

	Prefractionator	Main Column
Number of stages	17	36
Feed stage	9	–
Side stream stage	–	17
Interlinking stages	1/17	10, 11/23, 24
Distillate rate [lbmol/h]	86.92	40.45
Bottom rate [lbmol/h]	133.07	40.25
Feed flowrate [lbmol/h]	100.00	–
Reflux ratio [–]	0.39	2.78
Temperature of distillate [°F]	152.83	119.72
Pressure of top [psi]	21.08	21.08
Diameter [ft]	1.80	2.36
Liquid phase interlinking flow (FL1) [lbmol/h]	–	35
Liquid phase interlinking flow (FV2) [lbmol/h]	–	85

pared in terms of energy consumption, total annual costs, and thermodynamic efficiencies obtained by using steady state simulations. The second section presents the theoretical control properties obtained in the SVD analysis derived from open-loop dynamic simulation in Aspen Dynamics.

5.1 Steady State Analysis

Tabs. 2, 3, and 4 present the design parameters for the PTLK, APTLK, and PLTKP schemes, respectively, for the separation of case M1F1. It can be seen that the total number of stages in each distillation sequence is similar, as is the diameter of the shells, but the PTLKP sequence is, of course, more complex than the other two systems.

Tabs. 5–10 present energy consumptions, thermodynamic efficiencies, and total annual costs (see Appendix A and B) for

Table 3. Design variables, M1F1, alternative Petlyuk (APTLK).

	Main Column	Postfractionator
Number of stages	38	17
Feed stage	–	–
Side stream stage	18	–
Interlinking stages	6, 9/22, 27	1/17
Distillate rate [lbmol/h]	40.29	45.38
Bottom rate [lbmol/h]	40.41	31.27
Feed flow rate [lbmol/h]	100.00	–
Reflux ratio [–]	2.50	1.12
Temperature of distillate [°F]	119.72	149.49
Pressure of top [psi]	21.08	21.08
Diameter [ft]	2.21	1.23
Liquid phase interlinking flow (FL1) [lbmol/h]	53	–
Liquid phase interlinking flow (FV2) [lbmol/h]	43	–

Table 4. Design variables, M1F1, Petlyuk with postfractionator (PTLKP).

	Prefractionator	Main Column	Postfractionator
Number of stages	17	33	3
Feed stage	9	–	–
Side stream stage	–	–	2
Interlinking stages	1/17	10,11/23, 24, 14,15/17,18	1/3
Distillate rate [lbmol/h]	86.38	40.41	19.58
Bottom rate [lbmol/h]	141.62	40.29	10.12
Feed flowrate [lbmol/h]	100.00	–	–
Reflux ratio [–]	0.45	2.83	1.51
Temperature of distillate [°F]	161.30	119.71	180.21
Pressure of top [psi]	23.57	21.07	21.07
Diameter [ft]	1.81	2.36	0.84
Liquid phase interlinking flow (FL1) [lbmol/h]	–	38	–
Liquid phase interlinking flow (FV2) [lbmol/h]	–	90	–
Liquid phase interlinking flow (FL3) [lbmol/h]	–	30	–
Liquid phase interlinking flow (FV4) [lbmol/h]	–	19	–

the three complex distillation sequences. It can be noted that, for the case M1F1 (Tab. 5), the PTLKP sequence has the lowest energy requirement, but the APTLK presents the minimum total annual cost and the highest thermodynamic efficiency. This result is in agreement with the fact that the optimum scheme must be selected in terms of the total annual cost, because the same energy requirements in complex distillation sequences can be translated into different costs because of their dependence on the temperatures of the integrated distillation sequence reboilers.

For the case M1F2 (Tab. 6), the PTLK sequence presents the lowest energy consumption and the highest thermodynamic efficiency, but the ATPLK has the lowest total annual cost. Again, the ATPLK was optimal considering total annual costs.

For the case M2F1 (Tab. 7), the APTLK sequence presented the best energy requirement values, total annual cost, and thermodynamic efficiency. Once again, for the mixture M3F1 (Tab. 8), the APTLK sequence presented the lowest total annual cost, but not the best values of η and energy consumption. The analysis was conducted on the other cases (Tabs. 9 and 10), and it can be established that even in the cases where the PTLKP sequence has the lowest energy consumption, the cost of the extra shell may have a negative influence on the TAC, giving an advantage to other systems with only one lateral column.

An important remark can be made regarding the steady state design: in general, the complex distillation sequences involving only one dividing wall presented lower TAC in contrast to that obtained in the complex distillation sequence with two dividing walls. This can be explained in terms of the total traffic of liquids in the columns of the complex distillation sequences. According to Tabs. 2–4, the complex distillation sequences involving one dividing wall have total reflux ratios between 3 and 3.6, but the distillation sequence with two dividing walls presents a total reflux ratio of 5.0. It is important to highlight that the energy consumption increases as the reflux ratio increases.

1.2 Controllability Results

In order to conduct SVD analysis, open-loop transfer functions are required. In this study, step changes in the input variables were implemented and the open-loop dynamic responses were registered. The dynamic responses were adjusted to transfer functions and arranged into transfer function matrices. Tab. 11–13 present typical transfer function matrices for the case of separation of the mixture M1F1.

Fig. 4 presents the condition number for the case M1F1 in the frequency domain of interest, i.e., a clear trend in the parameters is observed. For this separation task, the PTLKP sequence shows the lowest value of γ^* , and according to Fig. 5, the highest value of σ^* . These results indicate that the PTLKP system has better theoretical control properties than the other two complex distillation sequences. It can be expected that the PTLKP option will present better closed-loop dynamic behavior for both set point tracking and load rejection in comparison to the other distillation sequences being studied. From a physical point of view, low values of the minimum singular

Table 5. Energy consumption, total annual cost, and thermodynamic efficiency (case M1F1).

Sequence	Energy consumption [Btu/h]	TAC [\$/yr]	η [%]
PTLK	1,772,695.32	297,969	31.07
APTLK	1,707,021.91	257,483	32.74
PTLKP	1,698,727.46	297,471	32.08

Table 6. Energy consumption, total annual cost, and thermodynamic efficiency (case M1F2).

Sequence	Energy consumption [Btu/h]	TAC [\$/yr]	η [%]
PTLK	2,031,240.06	328,168	17.69
APTLK	2,249,291.65	289,630	15.84
PTLKP	5,187,395.41	633,482	7.33

Table 7. Energy consumption, total annual cost, and thermodynamic efficiency (case M2F1).

Sequence	Energy consumption [Btu/h]	TAC [\$/yr]	η [%]
PTLK	4,738,309.88	891,355	13.18
APTLK	3,612,108.75	693,383	17.21
PTLKP	4,472,536.53	872,725	13.69

Table 8. Energy consumption, total annual cost, and thermodynamic efficiency (case M3F1).

Sequence	Energy consumption [Btu/h]	TAC [\$/yr]	η [%]
PTLK	4,391,690.02	728,735	14.02
APTLK	4,194,550.62	665,430	14.43
PTLKP	3,893,449.28	695,941	15.62

Table 9. Energy consumption, total annual cost, and thermodynamic efficiency (case M4F1).

Sequence	Energy consumption [Btu/h]	TAC [\$/yr]	η [%]
PTLK	2,126,220.73	342,783	16.19
APTLK	1,786,706.73	348,471	20.98
PTLKP	2,288,301.74	371,420	14.87

Table 10. Energy consumption, total annual cost, and thermodynamic efficiency (case M5F1).

Sequence	Energy consumption [Btu/h]	TAC [\$/yr]	η [%]
PTLK	9,886,134.58	1,410,484	3.99
APTLK	5,496,447.86	808,406	6.76
PTLKP	6,736,316.68	1,042,953	5.62

Table 11. Transfer function matrix for the Petlyuk column (M1F1).

$$\begin{array}{c}
 \begin{array}{ccc}
 & R & F & Q \\
 A & \frac{0.016}{(0.000830802s+1)(0.867304653s+1)} & \frac{0.0156}{0.828s+1} & \frac{-0.4448}{(0.402108168s+1)(0.286546099s+1)} \\
 B & \frac{0.0112}{(0.3323208s+1)(0.245259937s+1)} & \frac{0.0112}{(0.3323208s+1)(0.248259937s+1)} & \frac{0.0072}{0.032914516s+1} - \frac{0.1664}{1.268579447s+1} \\
 C & \frac{-0.0064}{(0.3323208s+1)(2.148732562s+1)} & \frac{-0.0064}{(0.3323208s+1)(2.148732562s+1)} & \frac{0.3616}{1.148937317s+1}
 \end{array}
 \end{array}$$

Table 12. Transfer function matrix for an alternative Petlyuk column (M1F1).

$$\begin{array}{c}
 \begin{array}{ccc}
 & R & F & Q \\
 A & \frac{-0.0536}{0.828s+1} & \frac{-0.0536}{0.828s+1} & \frac{-0.4232}{(0.328997592s+1)(0.229432964s+1)} \\
 B & \frac{-0.0132}{1.674505336s+1} & \frac{-0.0144}{2.8585872s+1} & \frac{0.0464}{0.3657s+1} - \frac{0.0436}{1.549011449s+1} \\
 C & \frac{0.0504}{1.210327489s+1} & \frac{0.0504}{1.210327507s+1} & \frac{0.408}{1.0602747s+1}
 \end{array}
 \end{array}$$

Table 13. Transfer function matrix for Petlyuk with postfractionator (M1F1).

$$\begin{array}{c}
 \begin{array}{ccc}
 & R & F & Q \\
 A & \frac{-0.0028}{0.101499992s+1} + \frac{0.0448}{0.692677085s+1} & \frac{-0.0076}{0.101499992s+1} + \frac{0.0496}{0.616482606s+1} & \frac{0.4552}{0.828s+1} \\
 B & \frac{-0.0016}{0.0828s+1} + \frac{0.0128}{1.505168s+1} & \frac{-0.0016}{0.0828s+1} + \frac{0.0128}{1.505168s+1} & \frac{0.0028}{0.013s+1} - \frac{0.1592}{1.324332747s+1} \\
 C & \frac{0.0016}{0.2s+1} - \frac{0.0212}{1.035s+1} & \frac{0.002}{0.2s+1} - \frac{0.0216}{1.035s+1} & \frac{0.3824}{1.100064825s+1}
 \end{array}
 \end{array}$$

value and high values of the condition number imply large movements in the control valves for changes in the set points and load rejection.

Figs. 6 and 7 display the results for the case M1F2. It can be seen in Fig. 6 that the APTLK and PTLKP sequences present similar values of the condition number for low and moderate frequencies, and these values are better than those obtained for the PTLK scheme. Similar results are obtained for the minimum singular value. Fig. 7 shows that the APTLK and PTLKP sequences present similar values for this parameter, and again, these values are better than those reported for the PTLK sequence. As a result, it can be expected that the PTLK sequence will have the worst closed-loop dynamic behavior.

For the mixture M2F1, Figs. 8 and 9 show a clear tendency for the complete range of frequencies. The APTLK system has the best control properties, i.e., the lowest condition number

values and the highest minimum singular value. In the case M3F1, according to Figs. 10 and 11, it can be expected that the PTLKP sequence will exhibit the best closed-loop dynamic performance, since it presents the lowest values for the condition number and the best minimum singular values. For the case M4F1 (Figs. 12–13), at low frequencies, the three systems have similar theoretical control properties, but, at higher frequencies, the PTLK sequence shows the best values for γ^* and σ_{∞} . Finally, for the mixture M5F1, Fig. 14 displays considerable variability of performance parameters, but at high frequencies, the APTLK sequence shows a major stabilization on the values of γ^* over the PTLK and PTLKP sequences. Similar results are obtained for the minimum singular value as indicated in Fig. 15, in which at low frequencies, the performance of the three systems is similar. However, at higher frequencies, the APTLK sequence begins to show the highest values of σ_{∞} .

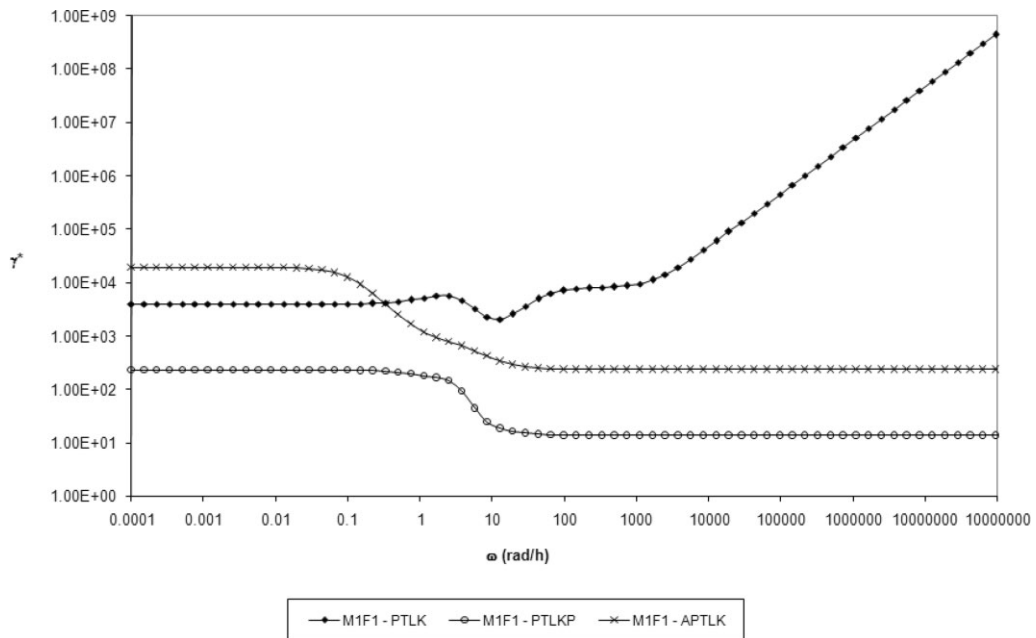


Figure 4. Condition numbers (M1F1).

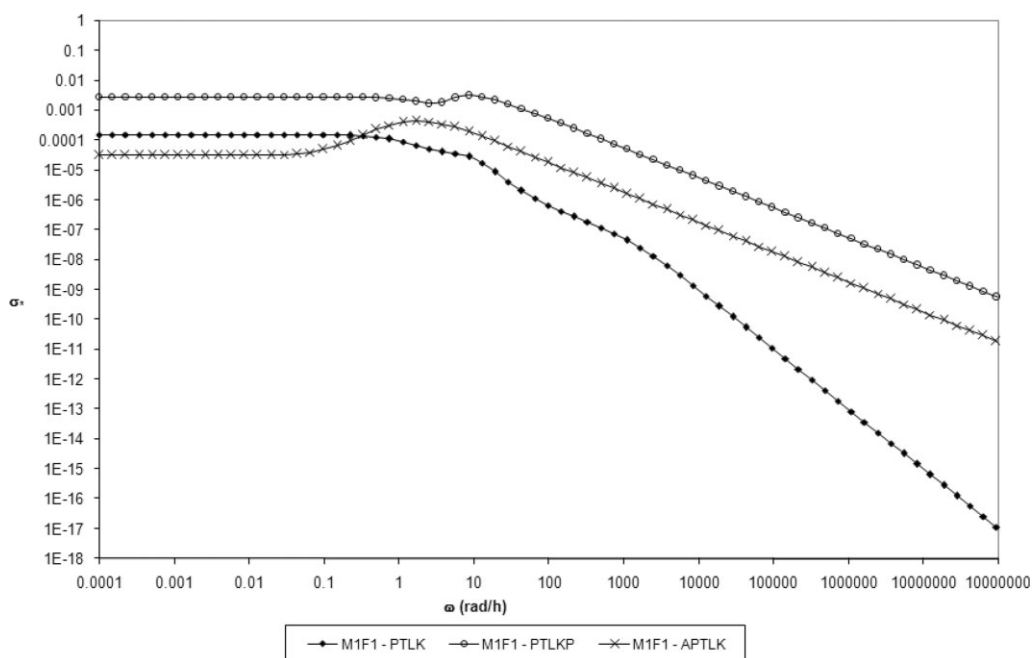


Figure 5. Minimum singular values (M1F1).

6 Conclusions

A design methodology for thermally coupled distillation sequences was presented. This methodology is based on stochastic optimization techniques, namely genetic algorithms.

Three thermally coupled schemes were tested, the traditional fully thermally-coupled Petlyuk scheme, an alternative scheme

with a postfractionator instead of the prefractionator, and a sequence with both pre- and postfractionator.

As can be seen from the results, the APTLK and PTLKP sequences (alternative Petlyuk and Petlyuk with postfractionator, respectively) showed better thermodynamic properties (i.e. heat requirements and thermodynamic efficiency) and lower total annual costs than the original Petlyuk column. Except for

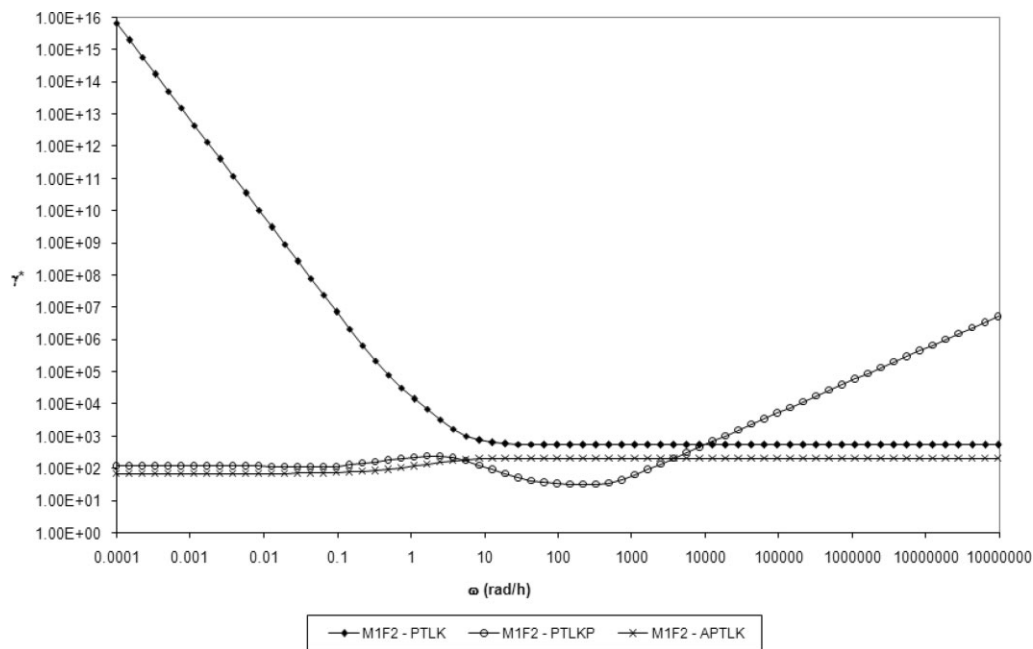


Figure 6. Condition numbers (M1F2).

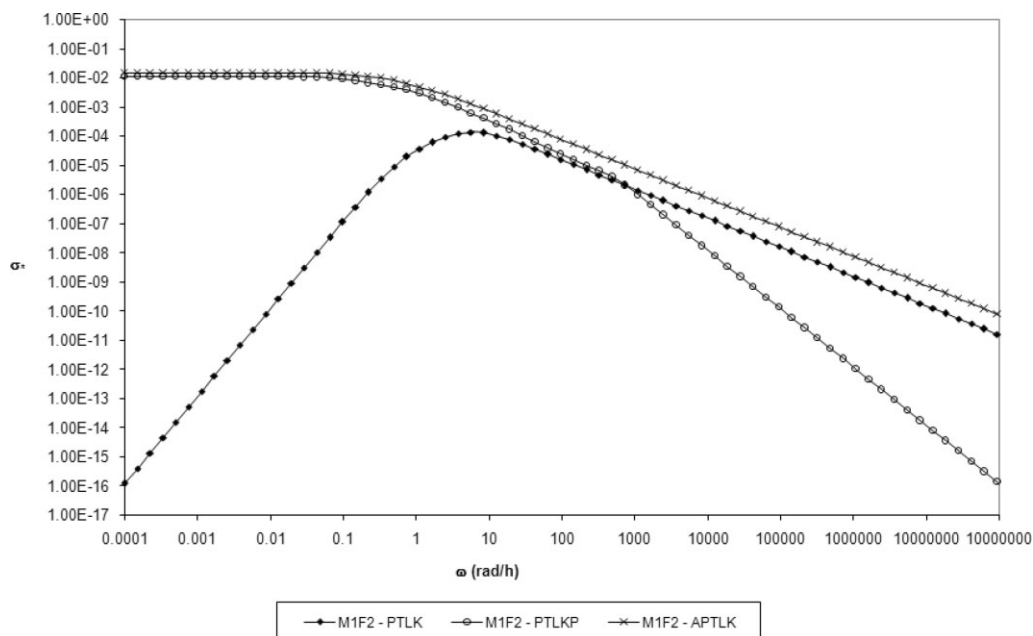


Figure 7. Minimum singular values (M1F2).

the case M1F2, a mixture of hydrocarbons with a composition high in the middle component.

For mixtures with a composition lower in the middle component, the PTLKP and the APTLK sequences showed low heat requirements and high thermodynamic efficiencies, but the APTLK has lower TAC because the PTLKP requires an extra column and the difference between energy consumptions is usually similar.

The design and optimization methodology used has proven to be an important tool to resolve these kinds of problems, producing results close to the global optimum and with low mathematical effort. Because of the complex nature of the studied systems, this rigorous simulation method is absolutely necessary to ensure that the best solution is chosen. Nevertheless, to make the final decision regarding which system is better, an analysis of both thermodynamic and control properties should be carried out.

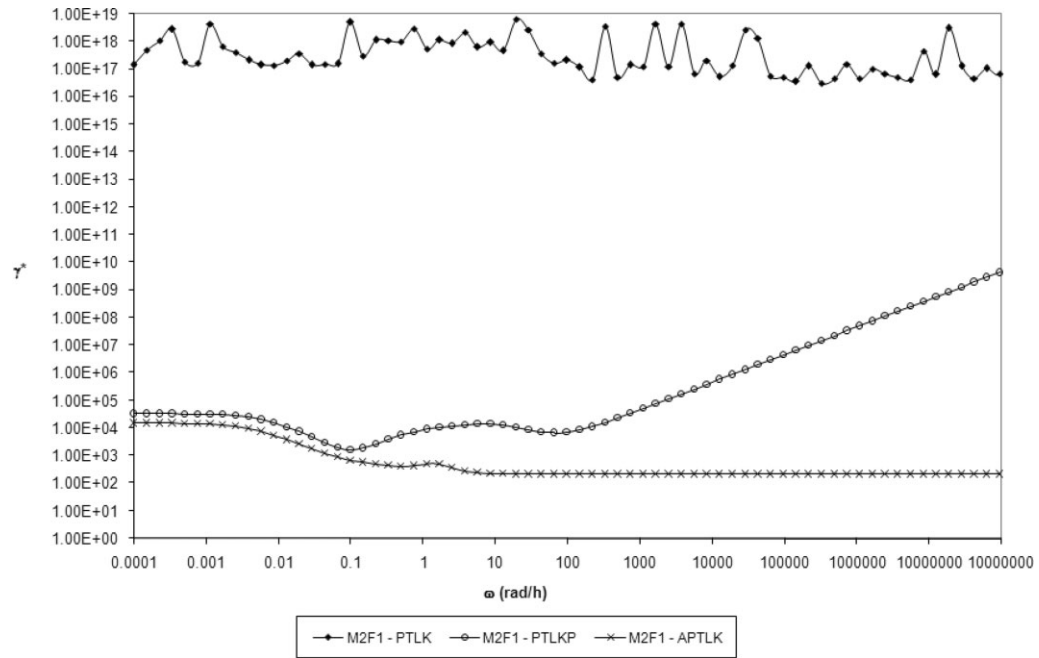


Figure 8. Condition numbers (M2F1).

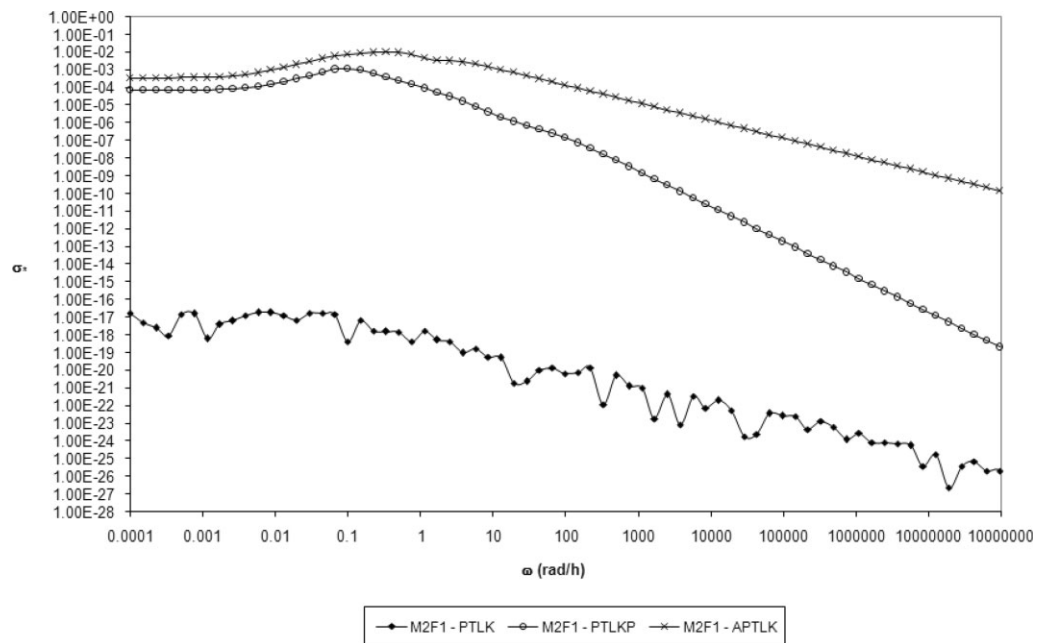


Figure 9. Minimum singular values (M2F1).

In accordance with theoretical control properties, it can be concluded that the distillation sequences other than the Petlyuk column presented the best values for condition number and minimum singular value. As a result, good dynamic closed-loop performance could be expected for these types of thermally coupled distillation sequences.

Acknowledgements

We acknowledge the financial support provided by Universidad de Guanajuato, CONACyT, and CONCyTEG (Mexico).

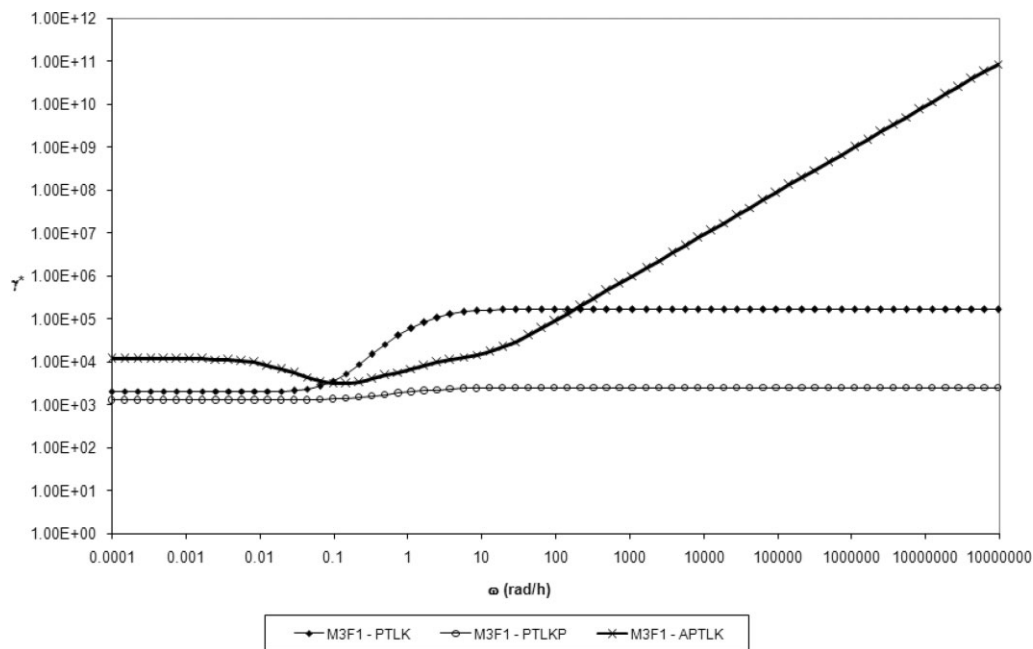


Figure 10. Condition numbers (M3F1).

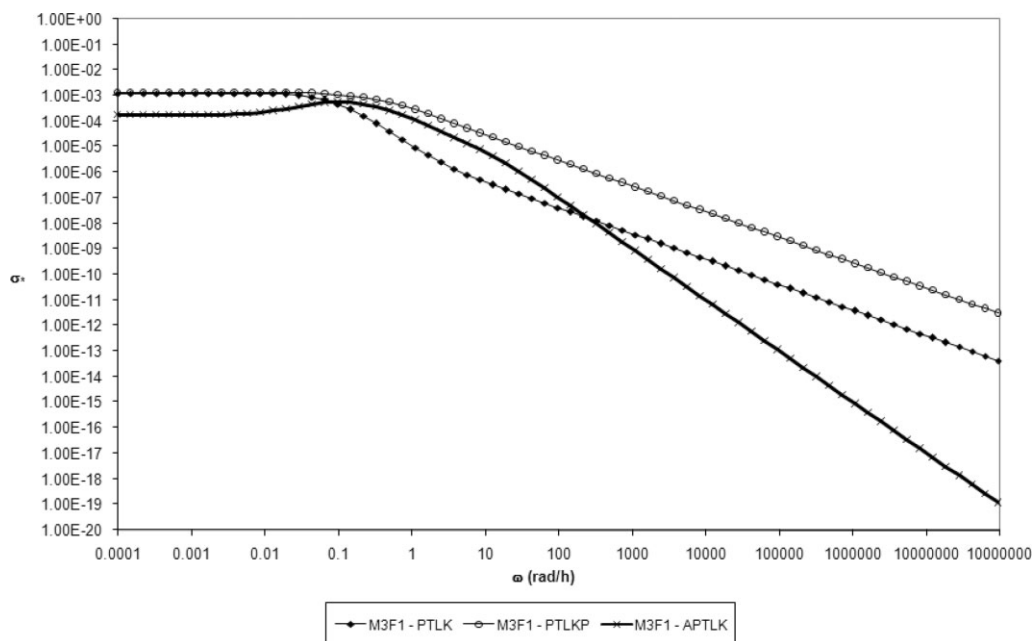


Figure 11. Minimum singular values (M3F1).

Appendix A

With the optimized designs of the dividing wall schemes, the thermodynamic efficiencies can be computed using the laws of thermodynamics. For this task, we used the equations reported in the textbook by Seader and Henley [37]. The equations are:

First Law of Thermodynamics:

$$\sum_{\text{out of system}} (nh + Q + W_s) - \sum_{\text{in to system}} (nh + Q + W_s) = 0 \tag{A.1}$$

Second Law of Thermodynamics:

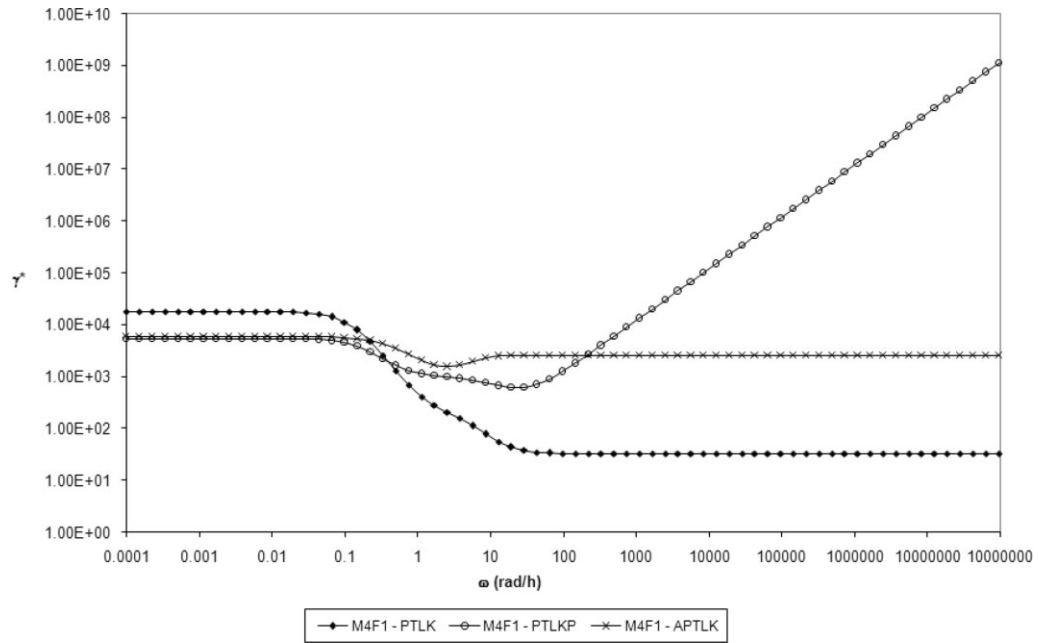


Figure 12. Condition numbers (M4F1).

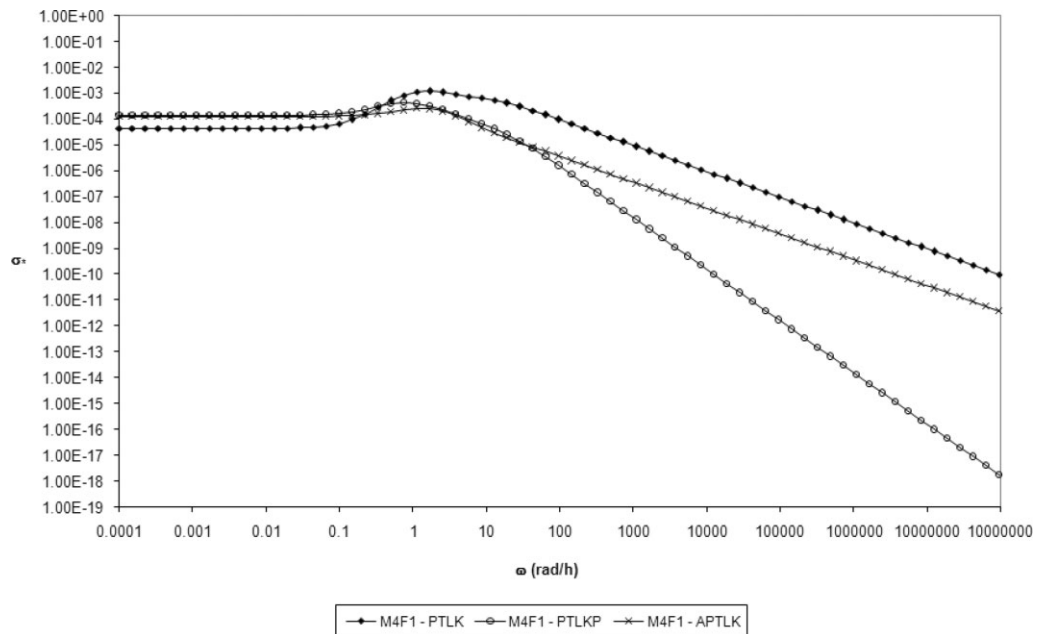


Figure 13. Minimum singular values (M4F1).

$$\sum_{\text{out of system}} (ns + Q/T_s) - \sum_{\text{in to system}} (ns + Q/T_s) = \Delta S_{\text{irr}} \quad (\text{A.2})$$

Exergy balance:

$$\sum_{\text{in to system}} \left[nb + Q \left(1 - \frac{T_0}{T_s} \right) + W_s \right] - \sum_{\text{out of system}} \left[nb + Q \left(1 - \frac{T_0}{T_s} \right) + W_s \right] = LW \quad (\text{A.3})$$

Minimum work of separation:

$$W_{\text{min}} = \sum_{\text{out of system}} nb - \sum_{\text{in to system}} nb \quad (\text{A.4})$$

Second law efficiency:

$$\eta = \frac{W_{\text{min}}}{LW + W_{\text{min}}} \quad (\text{A.5})$$

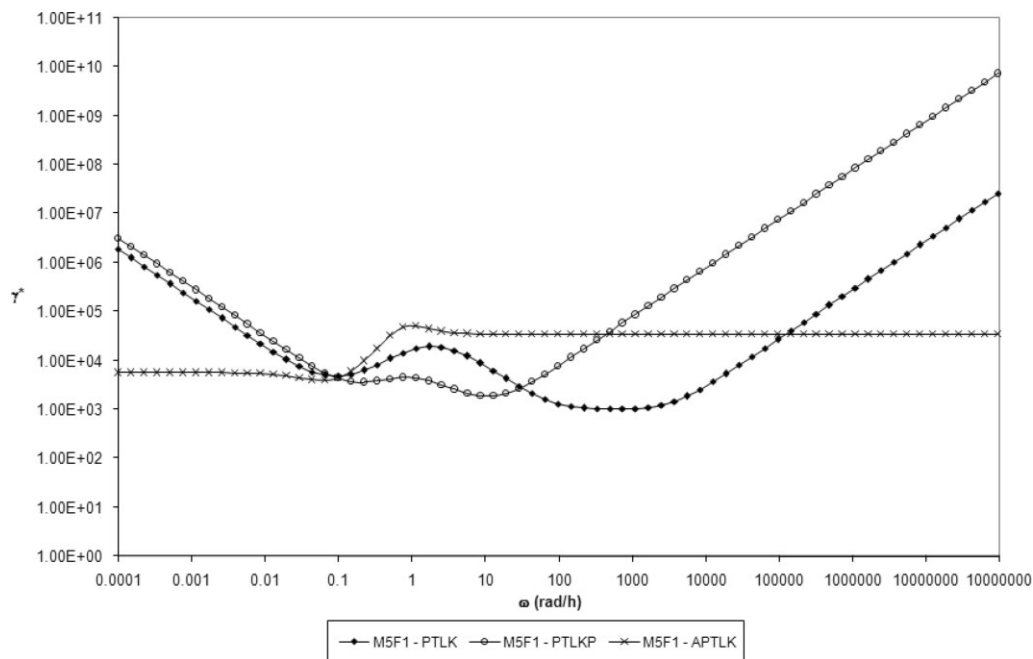


Figure 14. Condition numbers (M5F1).

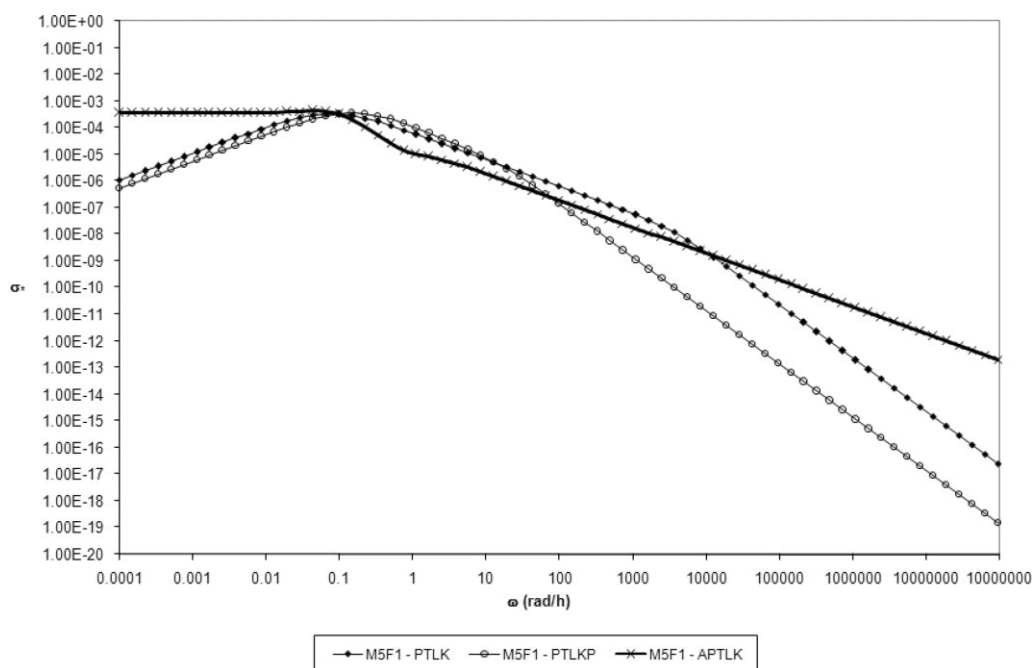


Figure 15. Minimum singular values (M5F1).

where $b = h - T_0 s$ is the exergy function, $LW = T_0 \Delta S_{irr}$ is the lost work in the system and η is the thermodynamic efficiency. The thermodynamic properties like enthalpies and entropies of the streams of the distillation sequences were evaluated through the use of the simulator of processes Aspen Plus 11.1™.

Appendix B

For a given number of theoretical trays, the Aspen Plus simulator calculates column diameter and height (for 24 in tray spacing) after converging for the selected valve tray column with 2 in weir height. Valve trays of Glitsch type are considered. The

costs of the distillation column (carbon steel construction) was estimated by the cost equations shown in Turton et al. [38], that are updated with the CEPCI (Chemical Engineering Process Cost Index). For comparison, a single value of CEPCI is selected (October, 2007), the value at the start of the year of this research. The total column cost is the sum of the installed cost of the column shell and the installed cost of column trays. On the other hand, the sizing and costing of heat exchangers were calculated. The cost of heat exchangers can be correlated as a function of the surface area, assuming shell and tube, floating head, and carbon steel construction. The installation prices are updated by the CEPCI index. The capital cost (purchase plus installation cost) is annualized over a period which is often referred to as plant lifetime:

$$\text{Annual capital cost} = \text{Capital cost} / \text{Plant life time} \quad (\text{B.1})$$

$$\text{Total annual cost (TAC)} = \text{Annual operating cost} + \frac{\text{Annual capital cost}}{\text{Plant life time}} \quad (\text{B.2})$$

Operating costs were assumed to be just utility costs (steam and cooling water).

Plant life = 5 years

Operating hours = 8400 h/yr.

Symbols used

b	[Btu/h]	exergy function
G	[-]	transfer function matrix
h	[Btu/lb-mol]	molar enthalpy
n	[lb-mol/h]	mole flow
Q	[Btu/h]	reboiler heat duty
S	[Btu/lb-mol °R]	molar entropy
TAC	[\$/yr]	total annual cost
T_0	[°R]	temperature of the surroundings
T_s	[°R]	temperature of the system
W_{\min}	[Btu/h]	minimum work for the separation
W_s	[Btu/h]	shaft work

Greek Symbols

σ^*	[-]	maximum singular value
σ_*	[-]	minimum singular value
γ^*	[-]	condition number
η	[-]	second law efficiency

References

- [1] R. Smith, B. Linhoff, *Chem. Eng. Res. Des.* **1988**, 66, 195.
- [2] P. Mizsey, Z. Fonyo, *Comput. Chem. Eng.* **1990**, 14, 1213.
- [3] C. Triantafyllou, R. Smith, *Trans. Inst. Chem. Eng. Part A* **1992**, 70, 118.
- [4] S. Hernandez, P. Pereira-Pech, A. Jimenez, V. Rico-Ramirez, *Can. J. Chem. Eng.* **2003**, 81, 1087.
- [5] M. Mascia et al., *Appl. Therm. Eng.* **2007**, 27, 1205.
- [6] O. Annakou, P. Mizsey, *Ind. Eng. Chem. Res.* **1999**, 38, 162.
- [7] G. Dünnebier, C. Pantelides, *Ind. Eng. Chem. Res.* **1999**, 38, 162.
- [8] M. A. Schultz et al., *CEP Magazine* **2002**, 98 (5), 64.
- [9] Y. H. Kim, *Chem. Eng. Proc.* **2006**, 45, 254.
- [10] E. A. Wolff, S. Skogestad, *Ind. Eng. Chem. Res.* **1995**, 34, 2094.
- [11] M. I. Abdul-Mutalib, R. Smith, *Trans. Inst. Chem. Eng. Part A* **1998**, 76, 308.
- [12] A. Jiménez, S. Hernández, F. A. Montoy, M. Zavala-García, *Ind. Eng. Chem. Res.* **2001**, 40, 3757.
- [13] J. C. Cárdenas et al., *Ind. Eng. Chem. Res.* **2005**, 44, 391.
- [14] J. G. Segovia-Hernández, S. Hernández, A. Jiménez, *Trans. Inst. Chem. Eng. Part A* **2002a**, 80, 783.
- [15] J. G. Segovia-Hernández, S. Hernández, V. Rico-Ramírez, A. Jiménez, *Comput. Chem. Eng.* **2004**, 28, 811.
- [16] J. G. Segovia-Hernández, S. Hernández, A. Jiménez, *Comput. Chem. Eng.* **2005a**, 29, 1389.
- [17] S. Hernandez et al., *Ind. Eng. Chem. Res.* **2005**, 44, 5857.
- [18] S. Hernandez, A. Jiménez, *Trans. Inst. Chem. Eng. Part A* **1996**, 74, 357.
- [19] N. Henderson, L. Freitas, G. M. Platt, *AIChE J.* **2004**, 50, 1300.
- [20] H. Yeomans, I. E. Grossmann, *Ind. Eng. Chem. Res.* **2000**, 39, 4326.
- [21] I. E. Grossmann, P. A. Aguirre, M. Barttfeld, *Comp. Chem. Eng.* **2005**, 29, 1203.
- [22] J. A. Caballero, I. E. Grossman, *Ind. Eng. Chem. Res.* **2001**, 40, 2260.
- [23] J. A. Caballero, I. E. Grossman, *Comput. Chem. Eng.* **2004**, 28, 2307.
- [24] J. Leboeiro, J. Acevedo, *Comput. Chem. Eng.* **2004**, 28, 1223.
- [25] J. Holland, *Adaptation in Natural and Artificial Systems*, Univ. of Michigan Press, Ann Arbor **1975**.
- [26] D. E. Goldberg, *Genetic Algorithms in Search, Optimization and Machine Learning*, Addison-Wesley, Massachusetts **1989**.
- [27] M. Gen, R. Cheng, *Genetic Algorithms and Engineering Optimization*, Wiley, Hoboken **2000**.
- [28] E. S. Fraga, T. R. Matias, *Comput. Chem. Eng.* **1996**, 20, 79.
- [29] S. V. Inamdar, S. K. Gupta, D. N. Saraf, *Chem. Eng. Res. Des.* **2004**, 82, 611.
- [30] K. H. Low, E. Sorensen, *Chem. Eng. Proc.* **2004**, 43, 273.
- [31] M. M. Barakat, E. S. Fraga, E. Sorensen, *Chem. Eng. Proces.* **2008**, in press. DOI: 20.1016/j.ccep.2008.01.005
- [32] A. Jiménez-Gutiérrez, A. Briones-Ramírez, C. Guitérrez-Antonio, in *Proc. of the European Symposium on Computer Aided Process Engineering-18 (ESCAPE-18)*, Lyon, France, **2008**.
- [33] C. A. Coello, *Civ. Eng. Environ. Syst.* **2000**, 17, 319.
- [34] V. C. Klema, A. J. Laub, *IEEE Trans. Autom. Control* **1980**, 25, 164.
- [35] H. S. Papastathopoulou, W. L. Luyben, *Ind. Eng. Chem. Res.* **1991**, 30, 705.
- [36] D. Tedder, D. Rudd, *AIChE J.* **1978**, 24, 303.
- [37] J. D. Seader, E. J. Henley, *Separation Process Principles*, 2nd ed., Wiley, Hoboken **2006**.
- [38] R. Turton, R. C. Bailie, W. B. Whiting, J. A. Shaeiwitz, *Analysis Synthesis and Design of Chemical Process*, 2nd ed., Prentice Hall, New Jersey **2004**.